ISSN: 0975-833X

Available online at http://www.journalcra.com

International Journal of Current Research
Vol. 14, Issue, 05, pp.21401-21409, May, 2022

DOI: https://doi.org/10.24941/ijcr.43494.05.2022

INTERNATIONAL JOURNAL OF CURRENT RESEARCH

RESEARCH ARTICLE

ATTENUATION OF MILLIMETRE WAVE BY SPHERICAL RAIN DROPS USING RAIN PARAMETERS IN YENAGOA

Aguiyi Nduka Watson, *Ayibapreye Kelvin Benjamin and Godday Biowei

Department of Electrical, Electronic Engineering, Niger Delta University

ARTICLE INFO

Article History:
Received 11th February, 2022
Received in revised form
20th March, 2022
Accepted 08th April, 2022
Published online 30th May, 2022

Key words:

Attenuation, Millimetre wave, Spherical, Rain drops, Drop size distribution

Corresponding Author:
Ayibapreye Kelvin Benjamin

ABSTRACT

In this paper, Mie theory was adopted to evaluate millimetre wave propagation in rain medium. This was to determine attenuation of propagating millimetre wave by rain drops in Yenagoa, Bayelsa State. We obtain Yenagoa climate weather averages for 2022 from weather.com and used these rain parameters to compute the effective permittivity of rain drops in Yenagoa by adopting Debye's model. The shape of rain drops was assumed to be spherical as drop diameter in Yenagoa is smaller than about $1.5\ mm - 2\ mm$. Drop size distribution (DSD) was evaluated using Marshall-Palmer's distribution and other distributions for different types of rain was studied. We observed that the all follow similar patterns. Finally, the specific attenuation by rain drops as a function of frequency and drop diameter was analysed and results obtained showed that the specific attenuation $\alpha\ (^{dB}/_{km})$ increases at smaller diameter rain drops and reduces for larger diameter rain drops. For smaller rain drops attenuation is due to absorption by water molecules with insignificant scattering by rain droplets while for larger rain drops there is significant scattering by rain drops with insignificant absorption of propagating millimetre waves by rain droplets. It was observed that the specific rain attenuation is constant at high frequencies. This is true for both day and night time as the maximum chord length d_{max} of raindrop becomes comparable to the wavelength λ in the rain medium which causes the raindrop to reradiate energy.

Citation: ***Ayibapreye Kelvin Benjamin, Aguiyi Nduka Watson and Godday Biowei.*** **2022.** "Attenuation of Millimetre Wave by Spherical Rain Drops using Rain Parameters in Yenagoa.". *International Journal of Current Research*, 14, (05), 21401-21409.

INTRODUCTION

The incessant demand for high bandwidth to meet current and future expectations of newer technologies associated with wireless networks and communication systems creates the overwhelming consideration for millimetre wave broadband (1). The 3-300GHz spectrum has been used extensively for the following applications which include AM/FM radio, Global Positioning System (GPS), satellite communication, high-definition TV, cellular communication, and Wi-Fi. However, the RF spectrum within millimetre wave has been underutilised for commercial wireless applications but the 60GHz band is available as an unlicensed spectrum and has raised attention in gigabit-per-second short-ranged wireless communication (2). The millimetre wave (mmW) band spans through 30-300GHz band of the RF spectrum. T. S. Zhouyue et.al asserted that the 3-30GHz band of the RF spectrum could be referred to as the mmW band as this frequency band has a corresponding wavelength between 1mm to 100mm. This band of frequencies comprise of the 3-30GHz super high frequency (SHF) and extremely high frequency (EHF) 30-300GHz. The SHF is popularly referred to as the Microwave frequency band while the EHF is referred to as the Millimetre wave band. Millimetre wave communications is rapidly becoming economically feasible and has led to the development of several standards, such as Wireless (High Definition) HD technology, ECMA-387, IEEE 802.15.3c, and IEEE 802.11ad (3). The Local Multipoint Distribution Service (LMDs) and 70/80/90 GHz bands launched by Federal Communications Commission (FCC) to provide fast data communication such as point-to-point wireless local area network, radio astronomy, inter-satellite link, high resolution radar, security screening, amateur radio, mobile backhaul, and broadband internet will sustain the potentials of full interference protection (4) (5).

The propagation of millimetre wave for extended capacity systems and indoor or similar complex propagation environment, particularly, in the 60GHz band have some imminent challenges such as multipath fading, potential line-of-sight blockage, power decay with distance, RF devices with low efficiency like multi-antenna arrays and power amplifiers with current technology. To achieve the expectations of millimetre wave technology it is significant to understand the propagation characteristics and challenges that it presents to network and system designers. Signals attenuates as they travel through indoor, outdoor and complex environments. This is due to atmospheric effects such as scattered and specular reflections, diffraction, refraction, interference (constructive and destructive) and absorption. Millimetre waves experience transmission loss due to free space path loss and other contributing factors such as atmospheric gaseous losses, foliage blockage, precipitation attenuation, scattering and diffraction by particles, buildings, hills, moving targets and stationary objects (6). The performance of communication systems is determined by radio propagation conditions. As electromagnetic waves propagate in the atmosphere (free space) they interact with particles (obstacles) during transmission which causes reflection, diffraction and scattering of the EM waves. Hydrometeors are water particles in solid and liquid form in the atmosphere. Some examples are hail, ice pellets, mist, rain, freezing rain, snow, ocean spray, clouds and fogs whose sizes are generally 1 μm or more in radium. Aerosols and hydrometeors are generally not of the same size, they are usually characterized by broad range of sizes. Electromagnetic properties, such as attenuation and depolarization, of a volume of aerosols or hydrometeors depend strongly on their size distributions, composition and shapes. At above $10\ GHz$, rain drops cause severe propagation loss due to absorption and scattering. Attenuation by rain drops is a very significant propagation effect and is vital for accurate prediction of millimetre wave propagation characteristics (7). Sheng et. al reported that various empirical and semi-empirical prediction models were used in evaluating attenuation by rain drops (8). In this paper, we predict the attenuation by raindrops using climate weather averages of 2022 in Yenagoa (12), Bayelsa State (See Table 1). Attenuation by rain drops depend on physical and electrical properties of rain drops such as drop size distribution (DSD), diameter (D) of rain drops, permittivity of water at specific temperature and propagating frequency.

Rain drops diameter range from $0.1mm - 8mm$ as drops with diameter larger than $8mm$ are unstable and breakup (8). Hence, high frequency approximation methods should be used at millimetre wavelength. From Table 1, we can see that the rain rate per hour is less than $1mm/hr$. With diameters less than $1.5mm - 2mm$, we assume that the shape of rain drops is spherical. In other cases, it is oblate ellipsoidal. The effective permittivity of water was calculated by Liebe's formula and the rain drop spectrum adopted is Marshall-Palmer spectrum.

Attenuation Due to Rain Drops: Due to the incessant growth in demand for additional communication capacity and emerging network capabilities such as 5G and next generation networks, there is need to harness higher frequency bands (above $10\ GHz)$ for efficient and effective communication systems. However, above $10\ GHz$ frequencies electromagnetic waves are prone to attenuation due to absorption by atmospheric particles which affects performance and reliability of radar and space communication links (9). These are particles such as rain, atmospheric gases, ice crystals, fog, snow and cloud. The significance of predicting the effects of atmospheric particles on the performance of communication systems cannot be taken for granted. This is due to their wide range of applications in weather monitoring and predictions. In this study, we shall investigate millimeter wave attenuation and phase shift on spherical rain drops. Here, we assume that the rain drops are spherical in order to evaluate its interaction with an incident EM field by adopting Mie theory. The aforementioned assumption is valid at low rain rate intensity. For high intensity rain, it is more realistic to model rain drops as oblate spheroids (9). In (9) the magnitude of a propagating EM wave through a homogeneous medium such as N identical spherical particles per unit volume with a distance z is expressed as $e^{-\alpha z}$, and α denotes the attenuation coefficient given by (10).

$\alpha = NQ_{ext}$ or

$$\alpha = \frac{N\alpha^2}{\pi} Re\ S(0) \quad (1)$$

Hence, attenuation of the EM wave is given as

$$A = 10\ log_{10} \frac{1}{e^{-\alpha z}} = \alpha z\ 10\ log_{10} e \quad (2)$$

or

$$A = 4.343\alpha z \qquad (in\ dB) \quad (3)$$

Therefore, attenuation per length (in $dB/m)$ is

$$A = 4.343\alpha$$

or

$$A = 4.343 \frac{\lambda^2 N}{\pi} \, Re \, S(0) \tag{4}$$

Likewise, the phase shift of the EM wave due to its interaction with the medium can be expressed as

$$\Phi = -\frac{\lambda^2 N}{2\pi} \, Im \, S(0) \qquad \left(in \frac{radians}{unit} length\right) \tag{5}$$

or

$$\Phi = -\frac{\lambda^2 N}{2\pi} \, Im \, S(0) \frac{180}{\pi} \qquad (in \, deg/m) \tag{6}$$

For an ideal rainfall, A and $\Phi$are expressed in terms of the $N(D)$for any given rain intensity. Rain DSD obtained using Laws and Parsons model are shown in Table 2. The effect of the rain DSD was evaluated for a particular rain rate R, with p as the percent of the total volume of water reaching the ground (see Table 2), which comprised of drops with diameters fall in the interval centered in $(d = 2a)$, the number of drops in that interval is given by

$$N_c = pN(D) \tag{7}$$

The total attenuation and phase shift over the entire volume become

$$A = 0.4343 \frac{\lambda^2}{\pi} \cdot 10^6 \sum pN(D) \; Re \, S(0) \left({}^{dB}/_{km} \right) \tag{8}$$

$$A = -\frac{9\lambda^2}{\pi^2} \cdot 10^6 \sum pN(D) \; Im \, S(0) \left({}^{deg}/_{km} \right) \tag{9}$$

λ denotes the wavelength in cm, $N(D)$ is the drop-size distribution with equal volume diameter $d \; per \; cm^3$ and $S(0)$ is the complex forward scattering amplitude obtained from Mie solution. The summations are taken over all drop sizes.

Table 2. Rain Rates for various (DSD) based on Laws and Parsons distribution (9)

Rain Rate $\left(\frac{mm}{hour}\right)$Drop0.25 1.252.505.0012.5 2550100 150 Diameter (cm)						Percent of total volume			
0.05	28.0	10.9	7.30	4.70	2.60	1.70	1.20	1.00	1.00
0.10	50.1	37.1	27.8	20.3	11.5	7.60	5.40	4.60	4.10
0.15	18.2	31.3	32.8	31.0	24.5	18.4	12.5	8.80	7.60
0.20	3.00	13.5	19.0	22.2	25.4	23.9	19.9	13.9	11.7
0.25	0.70	4.90	7.90	11.8	17.3	19.9	20.9	17.1	13.9
0.30		1.50	3.30	5.70	10.1	12.8	15.6	18.4	17.7
0.35		0.60	1.10	2.50	4.30	8.20	10.9	15.0	16.1
0.40		0.20	0.60	1.00	2.30	3.50	6.70	9.00	11.9
0.45			0.20	0.50	1.20	2.10	3.30	5.80	7.70
0.50				0.30	0.60	1.10	1.80	3.00	3.60
0.55					0.20	0.50	1.10	1.70	2.20
0.60						0.30	0.50	1.00	1.20
0.65							0.20	0.70	1.00
0.70									0.30

Modelling of Rain Drop Size Distribution and Refractive Index

Drop Size Distribution: The drop size distribution (DSD) is a measure of the ratio of the number of rain-drops to drop radius in a given volume. It is most often represented by an exponential distribution which implies a large number of small rain-drops and a few large ones. The exponential distribution is written as

$$n(D) = N_0 \exp(-\Lambda D) \tag{10}$$

With the drop diameter D in mm. The parameters N_0 $(mm^{-3-\mu} m^{-3})$ and Λ (mm^{-1}) depends on the rain rate R (mm/hr). In this paper, we employ the Marshall-Palmer (MP) distribution for evaluation of the attenuation of propagation electromagnetic field due to rain-drops.

Table 3. Shows expressions for N_0 and Λ applied in equation (10) describing the MP or other distributions used for different rain types.

Table 3. Different exponential DSD parameter (11)

Name	$N_0(mm^{-3-\mu}m^{-3})$	$\wedge(mm^{-1})$	$R\ (mm/hr)$
Marshall-Palmer	16×10^6	$8.2\times10^6R^{-0.03}$	<100
Laws and Parsons	$102\times10^6R^{-0.03}$	$7.6\times10^6R^{-0.03}$	Widespread, R low
Joss-Drizzle	60×10^6	$11.4\times10^6R^{-0.03}$	Convective, R high
Joss-Widespread	14×10^6	$8.2\times10^6R^{-0.03}$	<5
Joss-Thunderstorm	28×10^6	$6\times10^6R^{-0.03}$	≤150

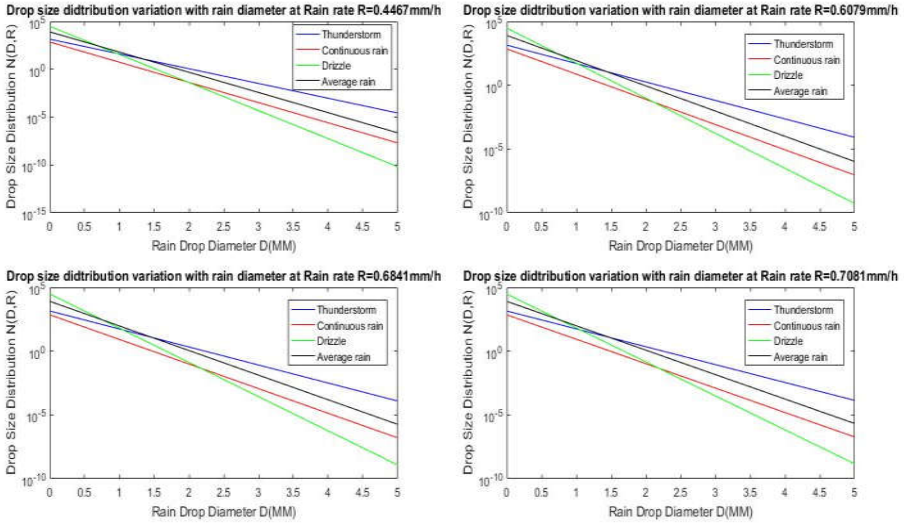

Figure 1. Variation of drop size distribution (DSD) with rain drop diameter at different rain rates for the months of (May, June, July and August as predicted for the year 2022)

Figure 1 and 2 show that for different rain types, the drop size distribution $N(D,R)$ reduces with increase in rain drop diameter for different rain rates R in Yenagoa.

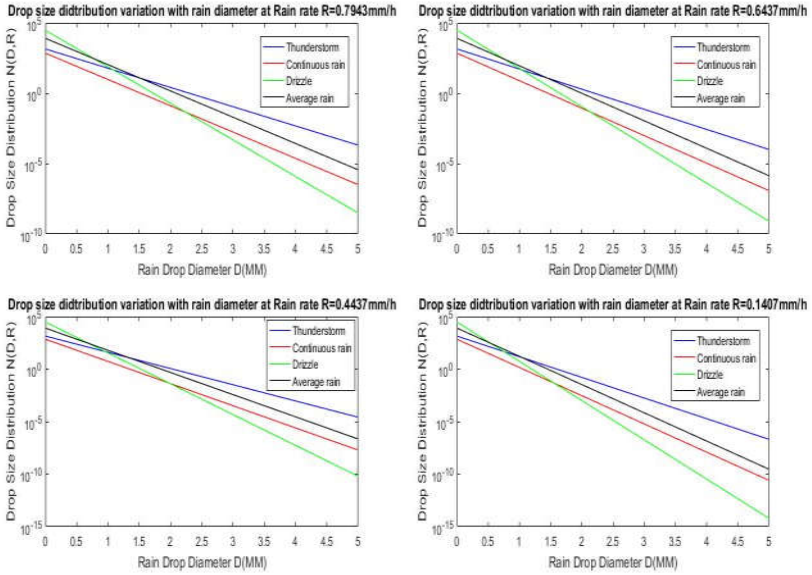

Figure 2. Variation of drop size distribution (DSD) with rain drop diameter at different rain rates for the months of (September, October, November and December as predicted for the year 2022)

Complex Permittivity of Rain drops: Propagation attributes of penetrating waves changes due to the refractive index m of a dielectric medium. In this paper, we adopt Debye model for the refractive index of water. This model shows the dependence of the refractive index on frequency and temperature. It is apparent that the frequency has more significant effect than temperature. Measurements at 60 GHzwere cited for two temperature ranges from 2℃ to 5℃ and from 25℃ to 28℃ showing negligible impact

on the refractive index by (Oguchi, 1983). Propagating electromagnetic waves are influenced by the permittivity ϵ_r of the medium and is related to the refractive index by

$$m = \sqrt{\epsilon_r} \tag{10}$$

The permittivity of pure water was evaluated from the standard Debye's model (Liebe, 1991) and verified with published measurements. It significantly alters wave properties inside a medium. The Debye model relates the permittivity of pure water as a function of frequency,

$$\epsilon_D\ (f) = \frac{\epsilon_0 - \epsilon_\infty}{1 + j\frac{f}{\gamma_D}} + \epsilon_\infty \tag{11}$$

with ϵ_0 as the static permittivity and ϵ_∞ the high frequency permittivity. γ_D is the relaxation frequency. The real and imaginary parts of the permittivity of pure water $\epsilon_r = \epsilon' - j\,\epsilon''$ of the Debye's model can be expressed as

$$\epsilon' = \epsilon_\infty + \frac{(\epsilon_s - \epsilon_\infty)\left[1 + (\lambda_s/\lambda)^{1-\alpha}\sin(\alpha\pi/2)\right]}{1 + 2(\lambda_s/\lambda)^{1-\alpha}\sin\left(\frac{\alpha\pi}{2}\right) + (\lambda_s/\lambda)^{2(1-\alpha)}} \tag{12}$$

and

$$\epsilon' = \epsilon_\infty + \frac{(\epsilon_s - \epsilon_\infty)\left[1 + (\lambda_s/\lambda)^{1-\alpha}\sin(\alpha\pi/2)\right]}{1 + 2(\lambda_s/\lambda)^{1-\alpha}\sin\left(\frac{\alpha\pi}{2}\right) + (\lambda_s/\lambda)^{2(1-\alpha)}} + \frac{\sigma\lambda}{18.8496 \times 10^{10}} \tag{13}$$

where σ is the conductivity, α denotes the spread parameter and λ_s is the relaxation wavelength which relates to γ_D by $\lambda_s = 2\pi/\gamma_D$.

Some variables that partially depend on temperature $T\ (°C)$ are

$$\sigma = 12.5664 \times 10^8\ 1/m \tag{14}$$

$$\alpha(T) = -\frac{16.8129}{T+273} + 0.0609265 \tag{15}$$

$$\epsilon_\infty\ (T) = 5.27137 + 0.0216474 - 0.00131198T^2 \tag{16}$$

$$\epsilon_s\ (T) = 78.54[1.0 - 4.579 \times 10^{-3}(T - 25.0) + 1.19 \times 10^{-5}(T - 25.0)^2 - 2.8 \times 10^{-8}(T - 25.0)^3] \tag{17}$$

$$\lambda_s(T) = 0.00033836 \exp\left(\frac{16.8129}{T+273}\right) cm. \tag{18}$$

(Liebe,1991) describe an advanced model plotted in figure 1, based on equation (11) with

$$\epsilon_0\ (\vartheta) = 77.66 - 103.3\vartheta. \tag{19}$$

$$\epsilon_\infty\ (\vartheta) = 0.066 \times \epsilon_0 \tag{20}$$

$$\gamma_D(\vartheta) = 20.27 + 146.5\vartheta + 314\vartheta^2 \tag{21}$$

ϑ denotes the temperature dependent parameter given by

$$\vartheta(T) = 1 - \frac{300}{273.15+T} \tag{22}$$

Figure 3 and 4 shows the relation between effective permittivity of rain medium as a function of temperature and frequency respectively. We can see that permittivity of rain rapidly decreases rapidly at low temperatures and decreases slowly at higher temperatures. Correspondingly, that permittivity of rain rapidly decreases rapidly at lower frequencies and decreases slowly at higher frequencies.

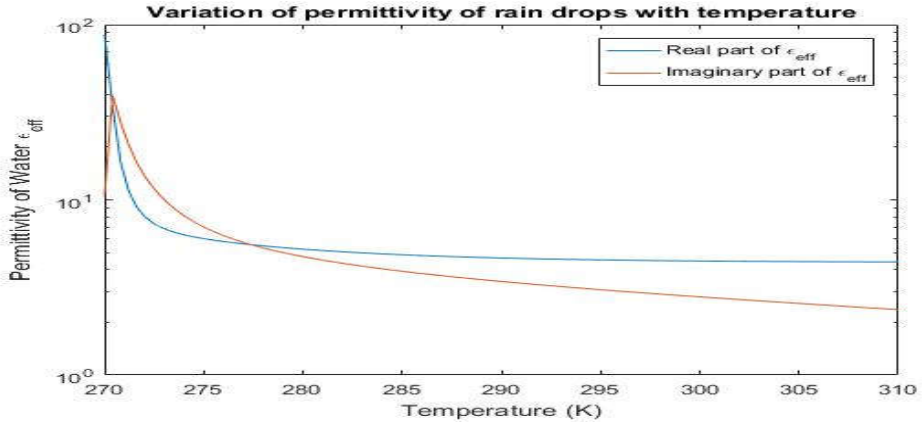

Figure 3. Effective permittivity of rain medium as function of temperature

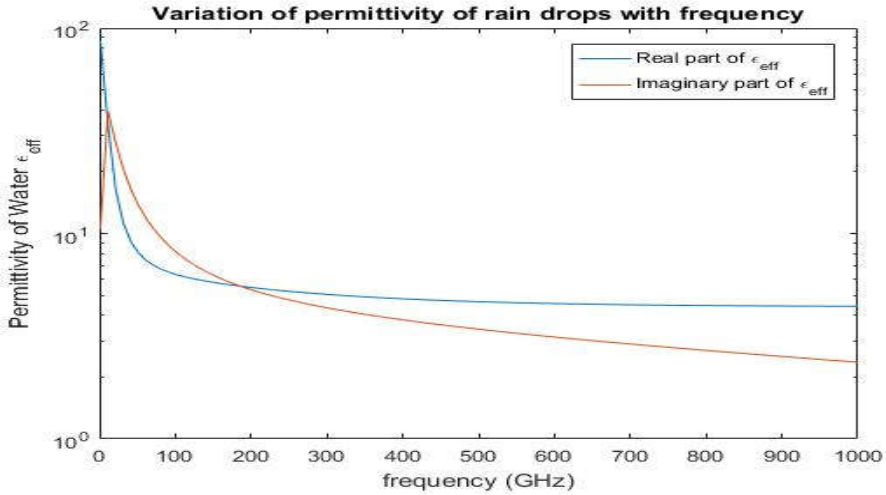

Figure 4. Effective permittivity of rain medium as function of frequency

This behaviour is similar in Figure 3 and 4. The real part of the effective permittivity decays slower as compared to that of the imaginary part. This shows that dielectric losses are the major contributors to scattering and absorption by rain drops in the rain medium. It is the same for Figure 3 and 4.

RESULTS AND DISCUSSION

Attenuation by raindrops at different drop size diameters and frequencies.

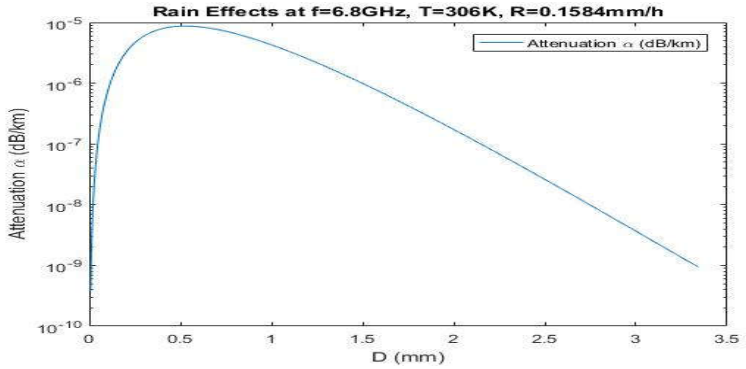

Figure 5. Specific rain attenuation as a function of drop diameter

Figure 5 and 6 illustrate specific attenuation due to rain effects at Wind Sat frequencies: 6.8 GHz and 10.7 GHz respectively. The specific attenuation varies with rain drop diameter $D\,(mm)$ at a given temperature of $T = 306K$ with rain rate $R = 0.1584\ {}^{mm}/_{h}$. We can see that the specific attenuation $\alpha\ ({}^{dB}/_{km})$ increases at smaller diameter rain drops and reduces for larger diameter rain drops.

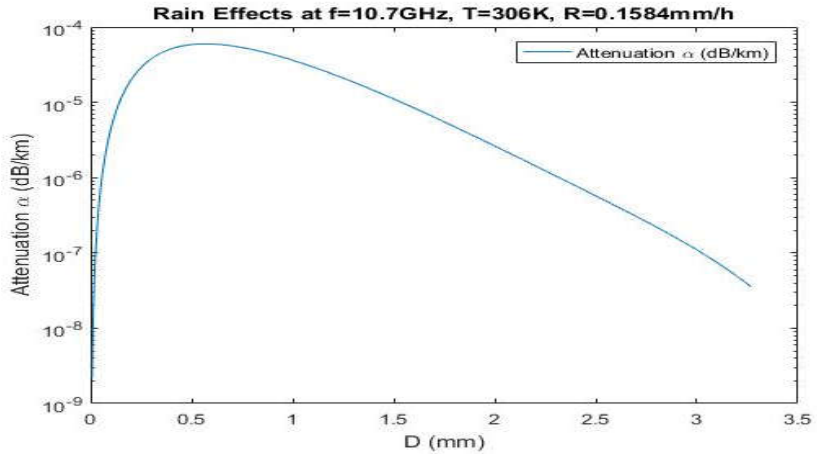

Figure 6. Specific rain attenuation as a function of drop diameter

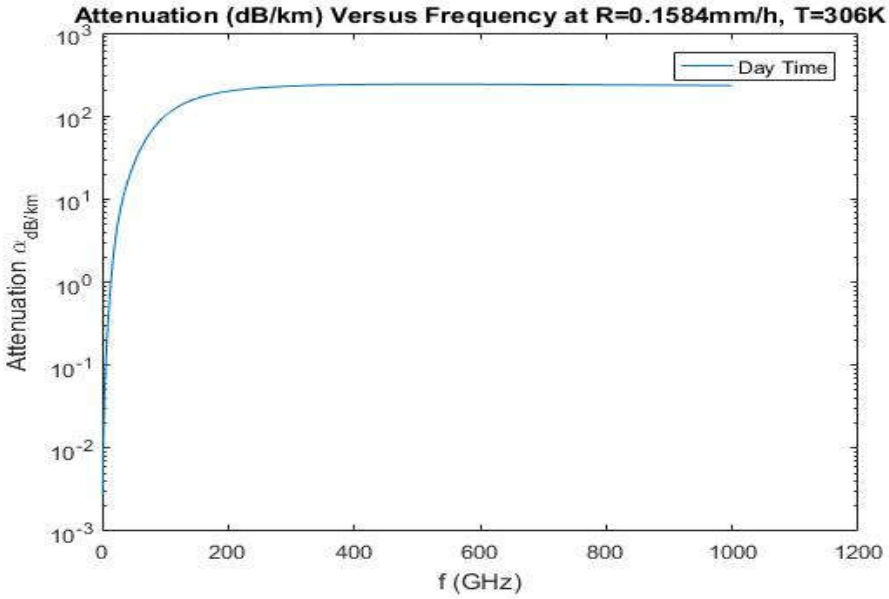

Figure 7. Specific rain attenuation as a function of frequency

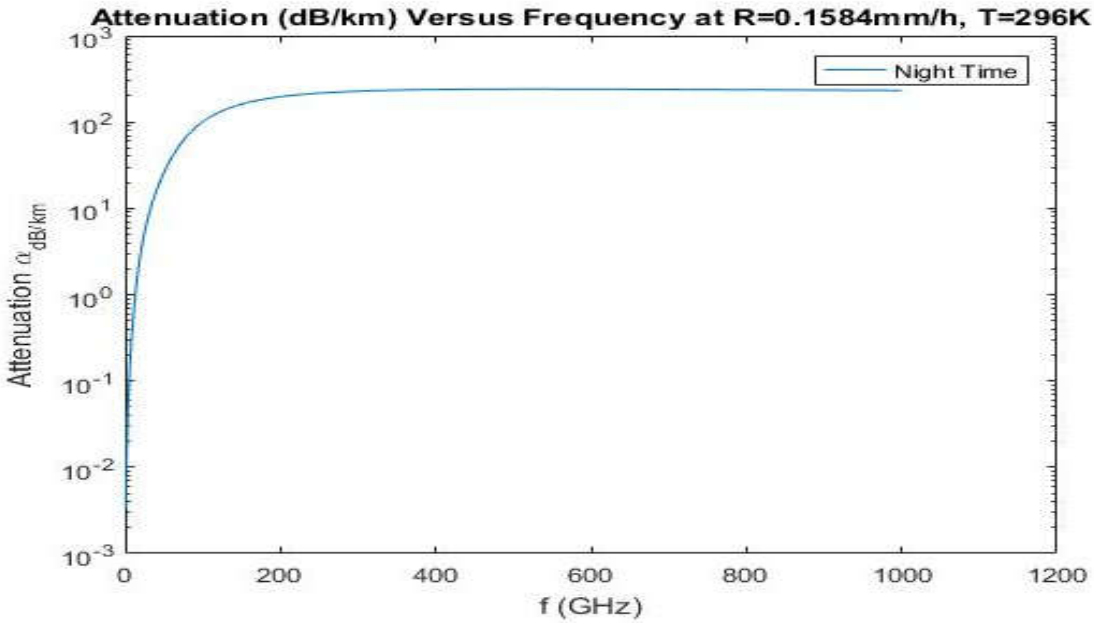

Figure 8. Specific rain attenuation as a function of frequency

For smaller rain drops attenuation is due to absorption by water molecules with insignificant scattering by rain droplets while for larger rain drops there is significant scattering by rain drops with insignificant absorption of propagating millimetre waves by rain droplets. The adopted Mie theory method used in investigating millimetre wave propagation in rain medium at rain rate $R = 0.1584\ {}^{mm}/_{h}$, which is the hourly rain rate for both day and night time in the month of January, 2022 in the city of Yenagoa, Bayelsa State (12). The drop size distribution was obtained using Marshall-Palmer's formular that is an exponential distribution. When compared with published results from (8), It was observed that it agrees with ITU-R method at microwave frequencies. It was observed that the specific rain attenuation is constant at high frequencies. This is true for both day and night time as the maximum chord length d_{max} of raindrop becomes comparable to the wavelength λ in the rain medium which causes the raindrop to reradiate energy. This energy that is reradiated relies on the closeness of the applied frequency f to the characteristic frequency f_r, at which reradiation is at maximum. At higher frequencies, the radiation rate is smaller and number of radiant raindrops increase for the same rainfall intensity. Hence, the total reradiated energy remains constant to the frequency of propagation electromagnetic wave. We can clearly see that Figure 7 to 10 follows similar pattern but the attenuation was higher for higher rain rate $R = 0.6079\ {}^{mm}/_{h}$, which is the rain rate for the month of June 2022 in Yenagoa.

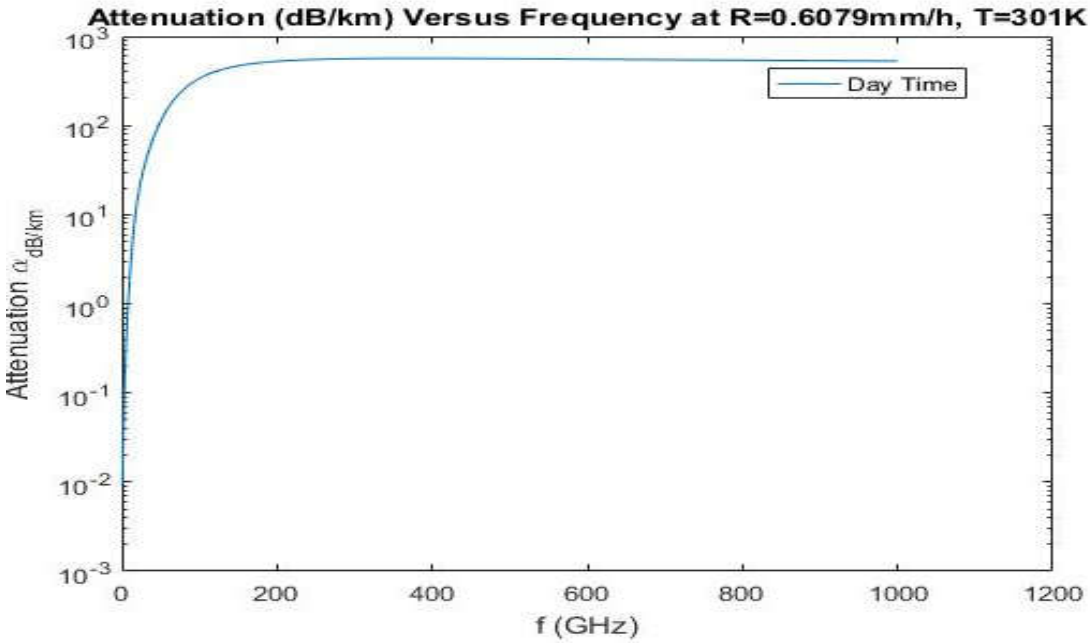

Figure 9. Specific rain attenuation as a function of frequency

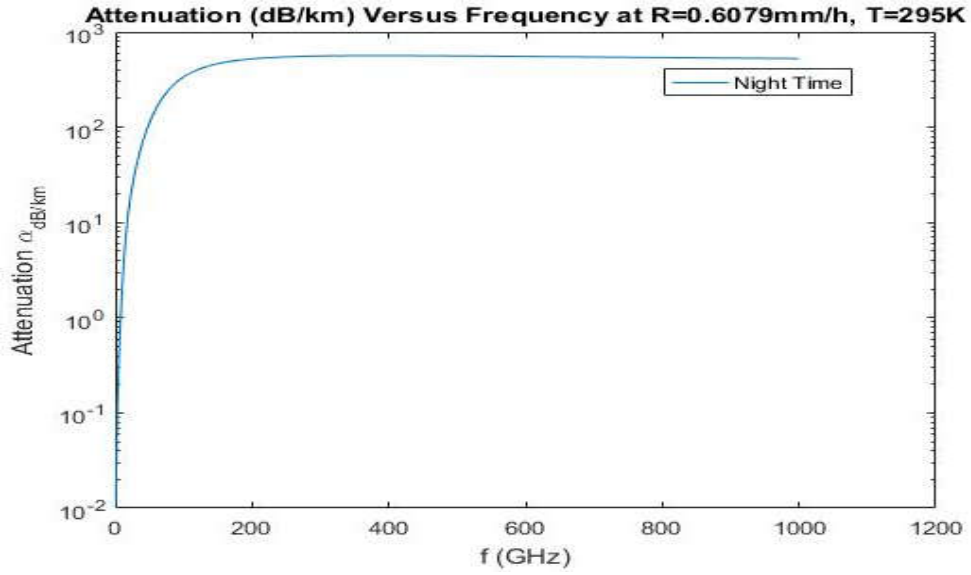

Figure 10. Specific rain attenuation as a function of frequency

CONCLUSION

This letter adopted Mie theory for spherical rain drops to evaluate rain attenuation due to millimetre wave propagation in rain medium. It uses weather parameters such as temperature $T\ (K)$, rain rate $R(mm/h)$ in Yenagoa, Bayelsa State to investigate extinction due to rain drops distribution in the atmosphere.

Debye's model for estimating effective permittivity as a function of temperature and frequency was used to determine the electrical properties of the rain medium. Drop size distribution of rain drops was obtained using Marshall-Palmer's distribution. The results obtained agrees with existing models such as ITU-R and parabolic equation (PE) models for millimetre wave propagation in rain medium as the specific attenuation increases for lower frequencies and is insensitive to the high frequencies as shown in Figure 9 and 10. This model provides an efficient numerical computation of millimetre wave interaction with spherical rain drops as drop diameters lies between $1.5\ mm - 2\ mm$.

REFERENCES

(1) F. Wang, and K. Sarabandi, "An Enhanced Millimetre-Wave Foliage Propagation Model", IEE Transactions on Antenna and Propagation, Vol.53, No.7, July 2005, pp. 2138-2145.
(2) Zhouyue Pi, and Farooq Khan, Samsung Electronics. "An Introduction to Millimetre-Wave Mobile Broadband and Systems", IEEE Communications Magazine, June, 2011.
(3) Eric Torkildson, Upamanyu Madhow, and Mark Rodwell, "Indoor Millimetre Wave MIMO: Feasibility and Performance", IEEE Transactions on Wireless Communications, Vol. 10. No.12, December, 2011.
(4) T. S. Rappaport et al.," Millimetre Wave Mobile Communications for 5G Cellular: It Will Work", IEEE Access, Vol. 1, pp.335-349, 2013.
(5) D.M. Pozar, "Microwave Engineering" Third Edition, ISBN 9812-53-186-6, John Wiley & Sons, 2005.
(6) I. Tardy and O. Grondalen, "On the role of future high frequency BFWA systems in broadband communication networks", IEEE Communication Magazine, Vol.42, pp.138-144, February, 2005.
(7) Adhikari, Arpita, Aniruddha Bhattacharya, and Animesh Maitra. "Rain-induced scintillations and attenuation of Ku-band satellite signals at a tropical location." *IEEE geoscience and remote sensing letters* 9, no. 4 (2012): 700-704.
(8) Sheng, Nan, Cheng Liao, Wenbin Lin, Qinghong Zhang, and Ruijie Bai. "Modeling of millimeter-wave propagation in rain based on parabolic equation method." *IEEE antennas and wireless propagation letters* 13 (2013): 3-6.
(9) Sadiku, Matthew NO. *Numerical techniques in electromagnetics*. CRC press, 2000.
(10) Hulst, Hendrik Christoffel, and Hendrik C. van de Hulst. *Light scattering by small particles*. Courier Corporation, 1981.
(11) Hipp, Susanne. "Electromagnetic Drop Scale Scattering Modelling for Dynamic Statistical Rain Fields." PhD diss., Technische Universität München, 2015.
(12) https://weather.com/Yenagoa Climate Weather Averages for 2022.